

# Receding-Horizon Adaptive Second-Order Sliding Mode Control for Doubly-Fed Induction Generator Based Wind Turbines

Carolina Evangelista<sup>1</sup>, Alessandro Pisano<sup>2</sup>, *Member, IEEE*, Paul Puleston<sup>1</sup> and Elio Usai<sup>2</sup>, *Member, IEEE*,

**Abstract**—In this paper a novel adaptive Second-Order Sliding Mode technique to optimise the efficiency of certain types of variable-speed wind turbines is developed and analysed. A revisited form of a recent adaptation algorithm is proposed to deal with the characteristics and control requirements of Wind Energy Conversion Systems (WECS), particularly model uncertainties and fast disturbances due to gusty wind effects. The revisited algorithm is based on appropriate receding-horizon adaptation time windows rather than on fixed, adjacent and non overlapping ones. This modification, which enhances the reactivity of the adaptation strategy against fast varying uncertainties, represents the main theoretical novelty of this work. The proposed approach is successfully used to control a Doubly-Fed Induction Generator based wind turbine topology proving its suitability for this application area. The novel adaptive controller is extensively assessed through computer simulations over a full-order realistic model of the WECS under study.

**Index Terms**—Wind Energy Conversion Systems; Conversion Efficiency Optimization; Nonlinear control; Second-order Sliding Mode Control; Adaptive Sliding Mode Control.

## I. INTRODUCTION

Wind Energy Conversion Systems (WECSs) are one of the most significant renewable clean energy sources, hence the development of dedicated controllers capable to improve their performance, lifetime and conversion efficiency is essential for the progress of this ever-evolving technology [1]. However, WECSs are complex systems involving nonlinear dynamics with strongly coupled internal variables, external disturbances and parameter uncertainties; consequently, advanced nonlinear control techniques are required to meet the challenge [2], [3].

Sliding Mode (SM) control has proven to be an especially apt technique capable to cope with the aforementioned complex characteristics. In fact, since its origins [4] [5], SM

control (SMC) has evolved into a robust and powerful design technique for a wide range of applications [6], [7], [8], [9]. The most distinguished aspect of SMC is the discontinuous nature of its control action, providing excellent system performance which includes insensitivity to certain parameter variations, rejection of matching disturbances, and finite-time convergence.

However, in practice, direct application of such discontinuous control effort is not adequate for some actual plants. Additionally, it can generate undesirable output chattering, which deteriorates the robustness of conventional SMC. To attenuate this problem, the concept of higher order sliding modes was introduced and, specifically, several Second-Order Sliding Mode (2-SM) algorithms were presented [10], [11], [12]. Since then, the number of publications on 2-SM theory and applications has grown exponentially (see [13], and references therein, for an overview).

Over the last decade, a number of interesting SMC solutions relying on adaptive mechanisms were presented. In [14] and [15] several adaptive first-order SMC algorithm are illustrated. The adaptive laws in [14] takes advantage of the possibility of achieving an online estimate of the equivalent control, through low-pass filtering of the discontinuous control, which allows one to modulate the amplitude of the switching control component. To overcome the difficulty of selecting the time constant of the filter, in [15] a different mechanism is devised which exploits the size of the boundary layer to adjust the discontinuous control effort. As a result, the discontinuous gain is kept at the smallest level that allows a given sliding-mode accuracy. Subsequently, a great deal of research has been devoted to develop different forms of adaptive 2-SM algorithms. In [16], an adaptive version of the Super-Twisting (ST) algorithm (see [10]) has been developed where the time-varying gains are only allowed to grow. In [17], a Lyapunov-based variable-gain ST algorithm was developed where the gains are adjusted on the basis of the currently measured states. The latter approach is applied in [18] and [19] to control different WECSs topologies with a generator similar to the one in the present paper. Very good results were obtained regarding conversion efficiency and chattering reduction. However, the computation of the appropriate bounding functions could become difficult (as it was in [19], with the MIMO WECS), or even impractical, if the system complexity is high.

Generalizing the methodology proposed in [14], the equivalent control principle has been exploited in [20], [21], [22] to develop adaptive ST algorithms. Particularly, the dual-layer adaptive concept of [22] provides a mechanism for adapting

A. Pisano and E. Usai gratefully acknowledge the financial support from the research projects “Modeling, control and experimentation of innovative thermal storage systems”, and “Development, design and prototyping of optimal management and control systems for micro-grids”, funded by Sardinia regional government, under grant agreements n. CRP-60193 and n. CRP-7733, respectively, and the project “RObust Decentralised Estimation fOR large-scale systems (RODEO)” funded by the Italian Ministry for Foreign Affairs under grant agreement n. PGR00152.

C. Evangelista and P. Puleston acknowledge the support of UNLP, CONICET and ANPCyT (Argentina), and Marie Curie FP7-2011-IIF, ACRES (299767/911767) (EU).

<sup>1</sup> C. Evangelista and P. Puleston are with the LEICI, Facultad de Ingeniería, Universidad Nacional de La Plata and CONICET, Argentina. {cae,puleston}@ing.unlp.edu.ar

<sup>2</sup> A. Pisano and E. Usai are with the Department of Electrical and Electronic Engineering, University of Cagliari, Cagliari, Italy {pisano,eusai}@diee.unica.it

both gains of the ST, whose structure is slightly modified, and provides global convergence guarantees which were not achieved in [20], [21]. In parallel, generalizing the adaptation mechanism introduced in [15], adaptive versions of the ST algorithm were presented, and experimentally verified, in [23], [24]. In contrast to our present proposal, a remarkable feature of such works is that they allow the uncertainty bounds not to be known a-priori. On the other hand, limitations of those algorithms include the fact that the size of the guaranteed invariant boundary layer is not evaluated. Furthermore, only sliding variable dynamics having relative degree one can be considered since the ST algorithm is used, in contrast to the adaptive 2-SMC approach of the present work where the relative degree can be one or two.

In [25], a continuous adaptive algorithm, providing finite time convergence to the second-order sliding mode for a class of nonlinear systems of relative degree two having uncertain parameters, was proposed. The Twisting (TW) algorithm (see [10]) has been also developed in adaptive forms in many recent works (see [26], [27], [28], [29], [30]). While all the mentioned works feature certain structural differences, from a general viewpoint the underlying Lyapunov-based adaptation principles are somewhat similar to that devised in [15], [24], with the main exception of [26] where a hybrid adaptation rule based on a sliding mode existence criterion has been employed. It should be mentioned that in the present paper we also take advantage of a sliding mode existence criterion which is, however, of completely different form as compared to the one in [26].

A readily implementable and straightforward adaptive 2-SM control (2-SMC) strategy was introduced in [31] to adjust the parameters of the TW algorithm. Instead of a Lyapunov-based gain adaptation (as in all the aforementioned works), this adaptation mechanism takes advantage of the inherent nature of the real (i.e., non ideal) SM regime, existing in actual systems operating at finite switching frequency. Its time-based adaptation policy simply depends on counting the zero-crossings of the sliding variable during appropriate adaptation time-windows. Then, the occurrence of the real SM behaviour is verified by checking whether such count is large enough according to a "SM existence" criterion. Like most of the existing adaptive 2-SMC schemes, the resulting adaptive controller is endowed with the capability of bidirectionally adjusting the discontinuous control gain, maintaining it at the minimum admissible level (rather than the worst-case over-conservative level, as in fixed-gain SM). Moreover, without adding a great degree of extra complexity to the real-time computations, the proposed adaptation preserves the robustness of its parental fixed-gain counterpart, while allowing an effective response to unexpected changes in the working conditions and performance enhancement of the controlled system (e.g., stress alleviation and chattering reduction). This adaptive 2-SMC algorithm has been applied in [32], [33] to adjust the parameters of the TW 2-SM algorithm [10] in robotic and automotive applications, respectively. Due to its computational simplicity, it proved to be specially suitable for implementation in standard microprocessor devices. In fact, it was experimentally verified in [32] by means of an industrial

manipulator. More recently [34], the same logic, combined with a switched adaptation algorithm (varying gains depending on the operating region), was applied to adjust the parameters of the Suboptimal 2-SM algorithm [12].

Driven by those encouraging results, the objective of this paper is to design, analyse and establish the feasibility of time-based adaptive 2-SM techniques to control variable-speed wind energy conversion systems, particularly Doubly-Fed Induction Generator (DFIG) based wind turbines. This type of turbines is an industry standard since the late 1990s, requiring only a slip power recovery fractional converter in the rotor (about 25%-30% of the total input mechanical energy), while the greater part of the power is fed to the grid directly from the stator. Efficiency increase and price reduction can be attained with such configuration.

In this context, to face the stringent specifications of the control problem in the WECSs scenario, where the uncertainties are subject to fast variations due to the wind effect, a revisited form of the time-based adaptation is sought. It is based on appropriate receding-horizon adaptation time windows rather than on fixed, adjacent and non overlapping ones, as in the previous proposals [32], [33], [34]. This modification, which enhances the reactivity of the adaptation strategy against fast varying uncertainties, represents the main theoretical novelty of this work. As compared to [34], therefore, we are not using here the switched adaptation paradigm (where the controller parameters are adjusted according to the current operating region in the state space) and, furthermore, receding horizon adaptation time windows are used here.

Preliminary results of the application of this novel adaptive 2-SMC proposal to a simple SISO WECS topology, based on an unidirectional DFIG and a dominant-dynamics reduced-order model, were presented in [35].

Then, in the present work, the potential of the proposal for variable speed WECSs is assessed by considering a versatile and comprehensive case-study of a variable-speed DFIG based topology with a bidirectional back-to-back converter drive in the rotor. The adaptive 2-SM MIMO controller design will be carried out by considering a simplified, reduced-order, mathematical model of the WECSs under study. The simulation studies, however, will be developed using the complete full-order model and in the presence of uncertainties, noise and other perturbations.

The plan of the paper is as follows: a general introduction to WECSs is given in Sect. II. Then, the case-study is addressed in Section III, where the control objectives are stated and the sliding manifold design is developed. Afterwards, Sect. IV presents the adaptive 2-SMC algorithm, together with the corresponding convergence proof. Section V presents some simulation results and the final Section VI draws some conclusions and perspectives for next research.

## II. WIND ENERGY CONVERSION SYSTEM BASICS

Typically, the operation of a DFIG based wind turbine can be divided into four zones depending on the wind speed (see Fig. 1) [36]. For wind speeds lower than a given cut-in speed  $\nu_{cut-in}$ , Zone I, the wind is not strong enough to move the

blades. Zone II, a.k.a. “partial load zone” ranges between the cut-in speed and the rated one  $\nu_r$ , and the control objective in such zone is energy conversion efficiency maximization. Usually, in this zone, the pitch angle of the blades is fixed at its optimum and the generator speed is varied by means of the DFIG rotor electric drive. In Zone III, or “full load zone”, which covers the interval from rated to cut-out wind speed  $\nu_{cut-out}$ , the controller must limit the power to its rated value. This can be accomplished either by controlling the electric drive, by adjusting the pitch angle, or by a combination of both. In Zone IV, above  $\nu_{cut-out}$ , the turbine should be turned out of the wind to prevent damages, so the generated power is zero.

The mechanical power a real turbine can instantaneously extract from the wind,  $P_t(t)$ , is a fraction of the total available wind power, determined by the power coefficient of the turbine,  $C_p(\lambda(t), \beta(t))$ , [36]:

$$P_t(t) = 0.5\pi\rho R^2 C_p(\lambda(t), \beta(t)) \nu^3(t), \quad (1)$$

where  $\nu(t)$  is the wind speed,  $\rho$  is the air density and  $R$  is the blades length.  $C_p(\cdot)$  depends on the shape and geometrical dimensions of the turbine, and it is a nonlinear function of the pitch angle of the blades  $\beta(t)$  and of the tip speed ratio  $\lambda(t) = \frac{\Omega_g(t)R}{k_{gb}\nu(t)}$ , where  $\Omega_g(t)$  is the angular speed of the generator rotor and  $k_{gb}$  is the transmission ratio of the speed multiplier (a rigid drive train is assumed). The curve  $C_p(\lambda, \beta)$  presents a unique maximum,  $C_{p\max} = C_p(\lambda_{opt}, \beta_{opt})$ , corresponding to the condition of maximum power extraction [3], [36].

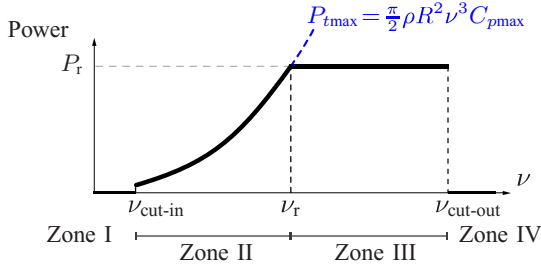


Figure 1. Zones of operation for a wind turbine.

The nonlinear differential equation that describes the mechanical dynamics of the system is

$$\dot{\Omega}_g(t) = \frac{T_t(\nu(t), \Omega_g(t)) + T_g(i(t))}{J}, \quad (2)$$

where  $J$  is the inertia of the whole combined rotating parts,  $T_t(\cdot) > 0$  is the torque exerted by the wind on the blades (referred to the high speed side by the transmission ratio of the speed multiplier, see appendix B), and  $T_g(\cdot) < 0$  is the electrical resistant torque of the generator, which depends on the currents  $i(t)$  of the DFIG (see (5) and (54)). Note that friction terms are neglected and fixed pitch-angle operation at  $\beta = \beta_{opt}$  is assumed. The expression of the turbine torque  $T_t = P_t/\Omega_g$  becomes, after simple manipulations:

$$T_t(\nu(t), \Omega_g(t)) = \frac{\pi\rho R^3}{2k_{gb}} C_t(\lambda(t)) \nu^2(t), \quad (3)$$

where  $C_t(\lambda) = C_p(\lambda, \beta_{opt})/\lambda$  is the torque coefficient modelled as  $C_t(\lambda) = \sum_{i=0}^3 c_i \lambda^i$  for some appropriate choice of

the coefficients  $c_i$ . From now on, the explicit dependence of the system's variables on the time variable will be skipped for the sake of notation simplicity.

### III. DFIG WITH BIDIRECTIONAL CONVERTER

The applicability of the proposed adaptive 2-SMC technique to DFIG-type WECSs is investigated by tackling a versatile DFIG topology, considering a bidirectional back-to-back converter in the rotor (see Fig. 2). This type of WECSs, largely used in variable-speed grid-connected applications, can operate in both sub- and super-synchronous speed ranges. When operating super-synchronously, electrical power is fed to the grid through both the stator and the rotor, whereas for sub-synchronous speeds, electrical power is injected into the rotor from the grid.

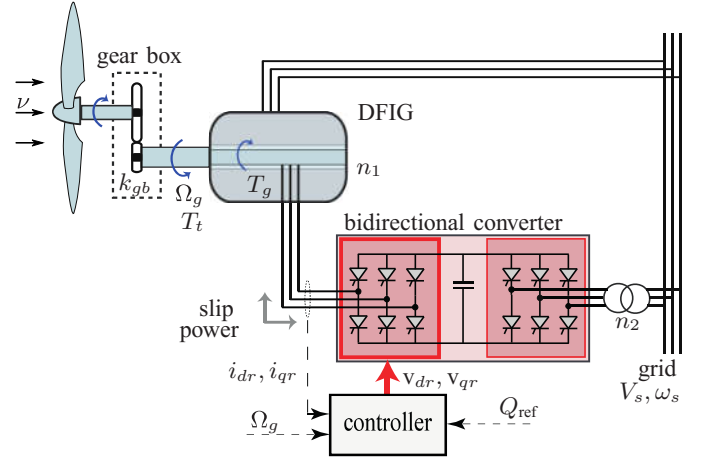


Figure 2. Schematic variable speed WECSs, based on a DFIG with a bidirectional back-to-back converter in rotor.

This configuration yields a multivariable system with two control inputs, i.e., the direct and quadrature rotor voltages, which makes it possible to pursue two independent objectives, for instance active and reactive power control. In this work, a comprehensive control strategy is developed for operation in both Zone II and Zone III, without resorting to wind-speed measurement.

A complete dynamical description of the system comprises five nonlinear differential equations (see appendix B). By means of some geometrical considerations (relative alignment between the rotating frames and the spatial fluxes) and a reasonable electric simplification (neglecting the stator resistance), a simplified third-order model can be obtained. This simplified description, whose variables are the direct and quadrature rotor currents and the mechanical rotation speed, is used for the control design, while the simulations for validation will be carried out using the full-order model. The reduced model is given by [37]:

$$\begin{aligned} \frac{di_{qr}}{dt} &= -\left(\frac{L_m V_s}{L_{eq}} + \omega_s i_{dr}\right) \left(1 - \frac{p}{\omega_s} \Omega_g\right) - \\ &\quad - \frac{R_r L_s}{L_{eq}} i_{qr} + \frac{L_s}{L_{eq}} v_{qr} \\ \frac{di_{dr}}{dt} &= i_{qr} (\omega_s - p \Omega_g) - \frac{R_r L_s}{L_{eq}} i_{dr} + \frac{L_s}{L_{eq}} v_{dr}, \end{aligned} \quad (4)$$



where  $v_{qr}$  and  $v_{dr}$  are the voltage control inputs and  $L_{eq} = L_s L_r - L_m^2$ , with  $L_m$  the magnetizing inductance, and the third equation corresponds to (2), with the following expression for the generator torque:

$$T_g(i_{qr}) = -\frac{3pL_m V_s}{2\omega_s L_s} i_{qr}. \quad (5)$$

#### A. Sliding manifold design

According to what has been stated above, two control objectives are tackled herein. The first one is to control the power extraction in both zones II and III, aiming to conversion efficiency optimization and power regulation, respectively, as shown in Fig. 1.

Given that it is assumed that no accurate wind speed information is available, the strategy for Zone II consists in indirectly attain conversion efficiency maximization ( $\lambda = \lambda_{opt}$ ) by tracking a time-varying optimum torque reference, which can be expressed as:

$$T_{opt}(\Omega_g) = \frac{\pi \rho R^5 C_{p \max}}{2k_{gb}^3 \lambda_{opt}^3} \Omega_g^2 = k_o \Omega_g^2, \quad (6)$$

where  $k_o = \pi \rho R^5 C_{p \max} / (2k_{gb}^3 \lambda_{opt}^3)$ .

On the other hand, in Zone III, when the wind speed is high, the limitation of power to the rated value,  $P_r$ , can be performed by tracking a time-varying torque reference:

$$T_r(\Omega_g) = \frac{P_r}{\Omega_g}. \quad (7)$$

The second control objective focuses on tracking an external reactive power reference in stator, in order to contribute compensating the grid power factor. The expression for the stator reactive power is [37]:

$$Q_s(i_{dr}) = \frac{3pV_s^2}{2\omega_s L_s} - \frac{3pL_m V_s}{2L_s} i_{dr}. \quad (8)$$

Then, the following two sliding variables are defined:

$$\sigma_1 = T_{ref} + T_g = T_{ref}(\Omega_g) - \frac{3pL_m V_s}{2\omega_s L_s} i_{qr}, \quad (9)$$

$$\begin{aligned} \sigma_2 &= Q_{ref} - Q_s = \\ &= Q_{ref} + \frac{3pL_m V_s}{2L_s} \left( i_{dr} - \frac{V_s}{\omega_s L_m} \right), \end{aligned} \quad (10)$$

where  $Q_{ref}$  is the external time-varying reference for the reactive power, and  $T_{ref}(\Omega_g)$  is the torque reference:

$$T_{ref}(\Omega_g) = \begin{cases} k_o \Omega_g^2, & \Omega_g \leq \Omega_{grated} \\ \frac{P_r}{\Omega_g}, & \Omega_g > \Omega_{grated} \end{cases}. \quad (11)$$

By virtue of (2), (4)-(8), the time derivatives of the sliding variables take the form

$$\begin{aligned} \dot{\sigma}_1(t) &= \frac{dT_{ref}}{dt} - \frac{dT_g}{dt} = \\ &= \frac{T_t + T_g}{J} \frac{dT_{ref}}{d\Omega_g} - \frac{3pL_m V_s}{2\omega_s L_s} \frac{di_{qr}}{dt}, \end{aligned} \quad (12)$$

$$\dot{\sigma}_2(t) = \dot{Q}_{ref} - \frac{dQ_s}{dt} = \dot{Q}_{ref} + \frac{3pL_m V_s}{2L_s} \frac{di_{dr}}{dt}. \quad (13)$$

Note that the control inputs  $u_1 = -v_{qr}$  and  $u_2 = v_{dr}$  enter in the right-hand side of (12)-(13) through the derivatives of the electrical currents, given in (4). Differentiating further (12)-(13) yields two expressions which can be written in the form:

$$\ddot{\sigma}_j(t) = f_j(\Omega_g, i_{qr}, i_{dr}, u_j, t) + g_j \dot{u}_j, \quad j = 1, 2, \quad (14)$$

highlighting the affine and decoupled dependence of each  $\ddot{\sigma}_j$  on the corresponding control derivative  $\dot{u}_j$ . 2-SMC design requires that the following inequalities hold for some constants  $G_{mj}$ ,  $G_{Mj}$  and  $F_j$ ,  $j = 1, 2$ :

$$0 < G_{mj} \leq g_j \leq G_{Mj}; \quad |f_j| \leq F_j. \quad (15)$$

To obtain appropriate theoretical bounds, the following expressions can be straightforwardly found by differentiation and adequate rewriting (arguments of functions  $f_j$  and  $g_j$  and time-varying signals are omitted for brevity):

$$\begin{aligned} f_1 &= -\frac{3p^2 L_m V_s}{2\omega_s L_s J} \left( i_{dr} + \frac{L_m V_s}{\omega_s L_{eq}} \right) \varphi_1 + \frac{d^2 T_{ref}}{dt^2} + \\ &+ \frac{3pL_m V_s (\omega_s - p\Omega_g)}{2\omega_s L_s} \left( \frac{L_s}{L_{eq}} v_{dr} - \frac{R_r L_s}{L_{eq}} i_{dr} + \right. \\ &+ \left. (\omega_s - p\Omega_g) i_{qr} \right) + \frac{3pL_m R_r V_s}{2\omega_s L_{eq}} \left[ \left( \frac{L_s}{L_{eq}} v_{qr} - \right. \right. \\ &- \left. \left. \frac{L_m V_s}{L_{eq}} + \omega_s i_{dr} \right) \left( 1 - \frac{p\Omega_g}{\omega_s} \right) - \frac{R_r L_s}{L_{eq}} i_{qr} \right], \end{aligned} \quad (16)$$

where  $\varphi_1 = \left( T_t - \frac{3pL_m V_s}{2\omega_s L_s} i_{qr} \right)$  and the second time derivative of  $T_{ref}$  depends on the zone of operation:

$$\frac{d^2 T_{ref}}{dt^2} = \begin{cases} \frac{2k_o}{J^2} \varphi_1 + \frac{2k_o \Omega_g}{J} \varphi_2, & \Omega_g \leq \Omega_{grated} \\ \frac{2P_r}{J^2 \Omega_g^3} \varphi_1 - \frac{P_r}{J \Omega_g^2} \varphi_2, & \Omega_g > \Omega_{grated} \end{cases}, \quad (17)$$

with

$$\begin{aligned} \varphi_2 &= \frac{\rho \pi R^3}{2k_{gb}} \left[ \left( 2c_0 \nu + \frac{c_1 R \Omega_g}{k_{gb}} - \frac{c_3 R^3 \Omega_g^3}{k_{gb}^3 \nu^2} \right) \dot{\nu} + \right. \\ &+ \left. \frac{\varphi_1}{J} \left( \frac{c_1 R \nu}{k_{gb}} + \frac{2c_2 R^2 \Omega_g}{k_{gb}^2} + \frac{3c_3 R^3 \Omega_g^2}{k_{gb}^3 \nu} \right) \right], \end{aligned} \quad (18)$$

$$\begin{aligned} f_2 &= \ddot{Q}_{ref} - \frac{3p^2 L_m V_s}{2L_s J} \varphi_1 - \frac{3pL_m L_s V_s}{2L_{eq}^2} v_{dr} - \\ &- \frac{3pL_m V_s}{L_{eq}} (\omega_s - p\Omega_g) \left[ \frac{L_m V_s (\omega_s - p\Omega_g)}{2\omega_s L_s} + \right. \\ &+ \left. R_r i_{qr} \right] - \frac{3pL_m V_s}{2} i_{dr} \left[ \frac{(\omega_s - p\Omega_g)^2}{L_s} - \right. \\ &- \left. \frac{R_r^2 L_s}{L_{eq}^2} \right] + \frac{3pL_m V_s}{2L_{eq}} (\omega_s - p\Omega_g) v_{qr}, \end{aligned} \quad (19)$$

$$g_1 = \frac{3pL_m V_s}{2\omega_s L_{eq}}, \quad (20)$$

$$g_2 = \frac{3pL_m V_s}{2L_{eq}}. \quad (21)$$

Then, to compute the bounding constants in (15), a worst-case analysis has been performed, considering maximum admissible intervals for the time-varying signals entering (16)-(21) (see Table I).

Table I

MAXIMUM RANGES FOR THE UNCERTAIN TIME-VARYING SIGNALS.

$\nu$ :	[6; 12] (m/s)	$i_{qr}$ :	[-80; 80] (A)
$\dot{\nu}$ :	[-0.5; 0.5] (m/s <sup>2</sup> )	$i_{dr}$ :	[0; 40] (A)
$\ddot{\nu}$ :	[-0.1; 0.1] (m/s <sup>3</sup> )	$v_{qr}$ :	[-300; 300] (V)
$\Omega_g$ :	[0.7 $\Omega_s$ ; 1.3 $\Omega_s$ ] (rad/s)	$v_{dr}$ :	[0; 30] (V)

Assuming uncertainties and other possible external disturbance effects as well, yields the following conservative theoretical bounds:

$$F_1 = 1.40316 \times 10^8; \quad F_2 = 5.86104 \times 10^{10}; \quad (22)$$

$$G_{m1} = 1.4754 \times 10^3; \quad G_{M1} = 2.2131 \times 10^3; \quad (23)$$

$$G_{m2} = 5.5620 \times 10^5; \quad G_{M2} = 8.3430 \times 10^5. \quad (24)$$

#### IV. ADAPTIVE SECOND-ORDER SLIDING MODE DESIGN

At this point, it is convenient to use a unified representation to write down each equation of the second-order nonlinear uncertain system (14) that, respectively, govern the dynamics of the sliding variables  $\sigma_1, \sigma_2$ . They take the following form

$$\begin{cases} \dot{z}_1^j(t) = z_2^j(t) \\ \dot{z}_2^j(t) = f_j + g_j v_j(t) \end{cases} \quad j = 1, 2, \quad (25)$$

where  $z_1^j(t) = \sigma_j(t)$ ,  $v_j(t) = \dot{u}_j(t)$  is the auxiliary control signal, and  $f_j(\cdot)$  and  $g_j(\cdot)$  are uncertain functions satisfying the inequalities stated in (15).

The two subsystems (25) will be now treated in a unified way, hence the subscript and superscript  $j$  in the corresponding functions and variables will be dropped for the simplicity sake. Therefore, from now on we let  $z_1(t) = \sigma(t)$ , and (25) and (15) will be represented, respectively, as

$$\begin{cases} \dot{z}_1(t) = z_2(t) \\ \dot{z}_2(t) = f(\cdot) + g(\cdot)v(t), \end{cases} \quad (26)$$

$$0 < G_m \leq g \leq G_M; \quad |f| \leq F. \quad (27)$$

To stabilize in finite time the uncertain ‘‘auxiliary system’’ (26)-(27), the following discontinuous algorithm, called Suboptimal algorithm, was proposed in the literature [12]:

$$v(t) = \dot{u}(t) = -\alpha(t)V \operatorname{sgn}(z_1 - z_{1M}/2) \quad (28)$$

$$\alpha(t) = \begin{cases} \alpha^* & \text{if } \left(z_1 - \frac{z_{1M}}{2}\right)(z_{1M} - z_1) > 0 \\ 1 & \text{otherwise} \end{cases} \quad (29)$$

where  $z_{1M}$  is the last extremal value of  $z_1$  (more precisely, the most recent local maximum, minimum, or horizontal flex point of the sliding variable, which can be evaluated with sufficient precision using measurements of  $z_1$  only [38]), and  $\alpha^*, V$  are tuning constants to be selected in accordance with the next inequalities

$$\alpha^* \in (0, 1] \cap \left(0, \frac{3G_m}{G_M}\right) \quad (30)$$

$$V > \frac{F}{G_m}\Phi, \quad \Phi = \max\left\{\frac{1}{\alpha^*}, \frac{4G_m}{3G_m - \alpha^*G_M}\right\} \quad (31)$$

Such constant-gain controller is modified by implementing a time-based adaptation mechanism which properly adjusts the gain parameter  $V$ , now denoted by  $V_{tb}(t)$ , thereby changing (28) into

$$v(t) = \dot{u}(t) = -\alpha(t)V_{tb}(t) \operatorname{sgn}(z_1 - z_{1M}/2). \quad (32)$$

The adaptation method that will be implemented is inspired by the one introduced in [31] for the TW 2-SM algorithm, and which was tailored to the Suboptimal algorithm in [34]. It is worth noting that in this paper we develop a different form of the adaptation mechanism as compared to that suggested in [34].

The basis of the adaptation logic is a suitable ‘‘sliding mode existence criterion’’. Receding horizon time intervals of fixed length  $T$  are considered of the form

$$\mathcal{T}_k \equiv [kT_a - T, kT_a] \quad k = k^*, k^* + 1, \dots \quad (33)$$

where  $T_a \ll T = k^*T_a$ ,  $k^* \in \mathbb{N}$ .  $T_a$  is the ‘‘adaptation period’’ of the gain-adjusting mechanism, and  $T$  is the ‘‘adaptation window’’. At the end of every interval  $\mathcal{T}_k$  the number of zero crossings of the quantity

$$\omega(t) = z_1(t) - z_{1M}/2 \quad (34)$$

during such an interval is computed. Note that function  $\omega(t)$  appears as argument of the sign function in the Suboptimal algorithm control law (32), hence when the corresponding number of zero crossings is sufficiently large it means that a real sliding-mode behaviour is occurring in a small vicinity of the sliding manifold. In turns, this implies that the control value is large enough to counteract the actual uncertainties. Thus, if the sliding-mode existence criterion is fulfilled, it is sensible to diminish the control gain at the end of the time interval. On the other hand, when the sliding-mode existence criterion is violated then the control gain is increased. Upper and lower saturation thresholds to the control gain  $V_{tb}(t)$  are also taken into account.

The time-based adaptation works as follows. The piece-wise constant gain  $V_{tb}(t)$  is defined according to

$$V_{tb}(t) = V_M^k, \quad t \in [kT_a, (k+1)T_a). \quad (35)$$

The amplitude parameter  $V_M^k$  is adjusted according to

$$\begin{aligned} V_M^i &= V_0, \quad i = 0, 1, 2, \dots, k^* - 1 \\ V_M^{k+1} &= \begin{cases} \max(V_M^k - \Lambda T_a, V_{\min}) & \text{if } N_{sw}^k(\omega) \geq N^* \\ \min(V_M^k + \Gamma T_a, V_{\max}) & \text{if } N_{sw}^k(\omega) < N^* \end{cases} \quad (36) \\ &\quad \text{for } k \geq k^*, \end{aligned}$$

where  $N_{sw}^k(\omega)$  is the number of sign commutations of  $\omega(t)$  in the interval  $\mathcal{T}_k$ , and  $N^*$  is an appropriate integer threshold. Roughly speaking, at the end of each time interval  $\mathcal{T}_k$  we decrement the time-based control magnitude  $V_{tb}(t)$  stepwise by  $\Lambda T_a$  if the sliding mode existence criterion is fulfilled, otherwise we increment it stepwise by  $\Gamma T_a$ . The adaptation logic also include lower and upper bounds for the control magnitude ( $V_{\min}$  and  $V_{\max}$ , respectively, the latter being a value fulfilling  $V_{\max} > \frac{F}{G_m}\Phi$ , where  $\Phi$  is defined in (31)).

Finally,  $V_0$  is an arbitrary nonnegative initial value, that can be selected smaller than  $V_{\max}$ . Note that the uncertainty bounds in (22)-(24) only affect the computation of the  $V_{\max}$  parameter.

We preliminarily recall a useful Lemma which will be invoked within the convergence proof of the algorithm.

**Lemma 1** [33] *Consider the second order auxiliary system (26) with the Suboptimal algorithm as control law, and let  $N_{sw}^k(\omega)$  be the number of zero crossings of  $\omega = z_1 - z_{1M}/2$  during the time interval  $\mathcal{T}_k$  of length  $T$ . If condition*

$$N_{sw}^k(\omega) \geq 3 \quad (37)$$

*is satisfied, and, additionally, there is  $a_1 > 0$  such that  $|\dot{z}_1(t)| \leq a_1 \forall t \in \mathcal{T}_k$ , then there exist constants  $\rho_1$  and  $\rho_2$ , independent of  $T$ , such that the next inequalities hold*

$$|z_1(t)| \leq \rho_1 T^2 \quad |z_2(t)| \leq \rho_2 T \quad \forall t \in \mathcal{T}_k \quad (38)$$

**Proof of Lemma 1.** See [33].

Rewrite the last equation of (25) as follows

$$\dot{z}_2(t) = g[\eta(t) + v(t)], \quad \eta(t) = \frac{f}{g}. \quad (39)$$

We assume that a positive constant  $P$  exists such that

$$\left| \frac{d}{dt} \eta(t) \right| \leq P, \quad t \geq 0 \quad (40)$$

We are now in position to state the next Theorem.

**Theorem 1:** *Consider system (26). Assume that the uncertain functions  $f(\cdot)$  and  $g(\cdot)$  satisfy the inequalities (27). Apply the time-based adaptive sub-optimal control law (29)-(32), (35)-(36), with (31) specified with  $V = V_{\max}$ , and*

$$\Lambda > 0, \quad \Gamma > \Lambda + 3P, \quad N^* \geq 3. \quad (41)$$

*Then, with large enough parameters  $T_a$  and  $T$ , the next relations are achieved after a finite-time transient for some positive constants  $b_1, b_2$*

$$|z_1(t)| \leq b_1 T^2, \quad |\dot{z}_2(t)| \leq b_2 T. \quad (42)$$

**Proof of Theorem 1.** See the Appendix.

**Remark 1:** It is worth to remark that the complicated relations (16)-(21) do not contribute to the real-time computations. In fact, they represent the drift and gain terms of the sliding variable dynamics (14), and such functions are only used off-line for computing the constants appearing in (22)-(24). The online computations to derive the actual value of the control input to be applied, to be made every  $T_a$ , are limited to the computation of the last extremal value  $z_{1M}$  (which just requires few subtractions and multiplications as explained in [38]), the computation of the current value of the gain  $V_M^{k+1}$  according to (36) and of the current value of the control input time derivative according to (29) and (32), and finally the discrete-time integration (e.g., by the Euler method). Thus, the computational burden of the proposed algorithm turns out to be particularly simple.

#### A. Practical tuning of the algorithm

Some guidelines for finding an effective tuning of the adaptive 2-SM controller parameters are given. This is useful, on one hand, because there is a large freedom in selecting their values, and on the other hand, because the restriction  $\Gamma > \Lambda + 3P$  in (41) is usually highly conservative. Thus, a “practically oriented” tuning procedure is helpful as a viable way to obtain the best performance from the proposed adaptive control algorithm.

In practice, due to discretization, measurement noise and/or actuator bandwidth limitations, the time interval between two successive adjustments of the control input has a lower threshold. According to this unavoidable implementation constraint, parameter  $T_a$  has to be chosen not less than such threshold.

Then, the pair  $(T, N^*)$  should be selected jointly. This is done by firstly choosing the interval length  $T$  as an integer multiple of  $T_a$  and then making an experimental (or simulative) test using the fixed-gain version of the controller and inspecting the actual “average” number of switches of the quantity  $\omega(t)$  along time windows of length  $T$ . This observed average value has then to be reduced (e.g., dividing it by two) to derive  $N^*$ . The rationale for this procedure is that the average switching frequency of the sliding variable will decrease when the magnitude of the discontinuous controller gain is diminished.

The  $\Lambda$  parameter is chosen arbitrarily, being convenient to use relatively small values to avoid an excessively “nervous” adaptation of the gain. Finally, parameter  $\Gamma$  must formally fulfil the inequality in (41), which is however unsuitable since the parameter  $P$  is usually highly conservative.  $\Gamma$  should be chosen large enough to allow a prompt restoring of the practical sliding mode condition when it is lost. In this sense, selecting its value between five and ten times the value of  $\Lambda$  represent a reasonable choice.

## V. SIMULATION RESULTS

In this section, the unified notation adopted in Sec. IV is dropped. Thus, parameters  $V_0, V_{\max}, V_{\min}, \Lambda, \Gamma, N^*$  from (36) associated to sliding variable  $\sigma_j, j = 1, 2$ , and its corresponding controller  $u_j$ , will now be explicitly denoted  $V_{0,j}, V_{\max,j}, V_{\min,j}, \Lambda_j, \Gamma_j$  and  $N_j^*$ , respectively.

The performance of the proposed adaptive 2-SM control system is assessed via computer simulations. The simulation runs correspond to 10 minutes of system operation, using the wind profile shown in Fig. 3, which spans over both the zones II and III.

The simulated system is a three-bladed horizontal-axis WECSs based on a DFIG with a bidirectional converter and a rated power of 37kW. Its full-order model is used in the present section (the model and nominal parameters can be found in the appendix). In addition, a friction torque disturbance was applied at  $t \geq 300$ sec, which is shown in the upper plot of Fig. 4, and time-varying fluctuations of the grid line voltage and frequency have been considered (see the lower plot of Fig. 4). All system parameters have been also subject to variations up to 20% with respect to their nominal values.

The plan of the simulation analysis is as follows. Firstly, in Subsec. V-A, a comparison between the fixed-gains 2-SM

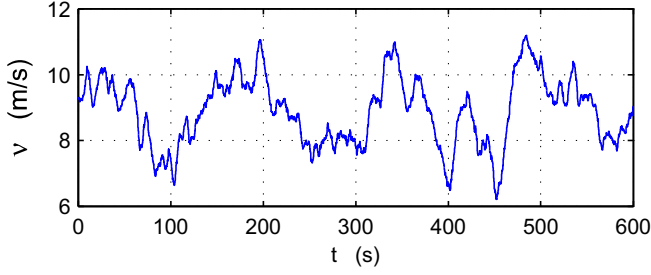


Figure 3. Wind speed profile.

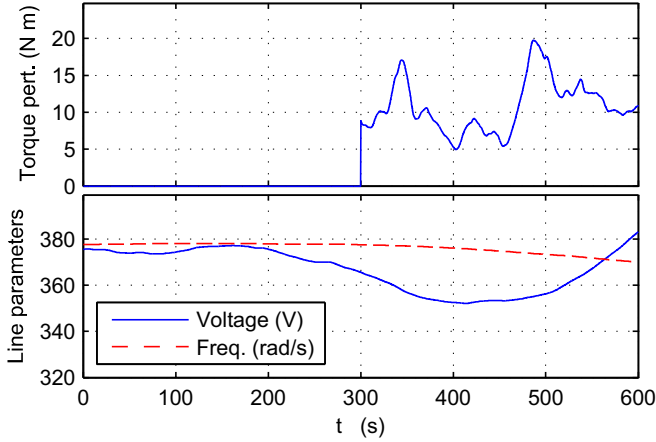


Figure 4. Upper plot: Variations of the grid line voltage and line frequency. Lower plot: Torque disturbance.

controller (28)-(29) and the adaptive version proposed herein will be presented in the absence of noise. Subsequently, in Subsec. V-B, significant implementation issues such as the presence of measurement noise and the sensitivity of the adaptive controller against the chosen sampling period will be investigated.

#### A. Adaptive versus fixed-gains 2-SM controllers

To compare both controllers, the values of all the parameters were determined in the first place. The computation of the fixed-gains parameters ( $V_1$ ,  $\alpha_1^*$ ,  $V_2$  and  $\alpha_2^*$ ) based on the theoretical bounds introduced in (22)-(24), provides extremely large values, not feasible for implementation as they will cause unacceptable chattering in the fixed-gains realization of the controller. After further heuristic refinement the following parameters, suitable for practical use, have been employed:

$$\alpha_1^* = 0.54; \quad V_1 = 300. \quad \alpha_2^* = 0.54; \quad V_2 = 30. \quad (43)$$

Regarding the proposed adaptive 2-SM controller, the explicit expressions of the control law, where  $u_1 = -v_{qr}$  and

$u_2 = v_{dr}$ , are the following:

$$\begin{aligned} \dot{u}_j(t) &= -\alpha_j^*(t) V_{tb,j}(t) \operatorname{sgn}(\sigma_j - \sigma_{jM}/2) \\ V_{tb,j}(t) &= V_{Mj}^k, \quad t \in [kT_a, (k+1)T_a) \\ V_{Mj}^i &= V_{0,j} \quad i = 0, \dots, k^* - 1 \\ V_{Mj}^{k+1} &= \begin{cases} \max(V_{Mj}^k - \Lambda_j T_a, V_{\min,j}) & \text{if } N_{sw}^k(\omega_j) \geq N_j^* \\ \min(V_{Mj}^k + \Gamma_j T_a, V_{\max,j}) & \text{if } N_{sw}^k(\omega_j) < N_j^* \end{cases} \\ &\quad \text{for } k \geq k^*, \end{aligned} \quad (44)$$

where  $N_{sw}^k(\omega_j)$  are the number of sign commutations of  $\omega_j(t) = \sigma_j - \frac{\sigma_{jM}}{2}$  in the intervals  $\mathcal{T}_k \equiv [kT_a - T, kT_a]$ , as defined in (33). The practical tuning procedure previously outlined in the Subsection IV-A has been followed and its parameters were finally set as follows

$$\begin{aligned} T_a &= 1\text{ms}; & T &= 200T_a; \\ N_1^* &= 6; & \Lambda_1 &= 1.2; & \Gamma_1 &= 9; \\ V_{\max,1} &= V_1; & V_{\min,1} &= 0.1; & V_{0,1} &= 100; \\ N_2^* &= 4; & \Lambda_2 &= 0.2; & \Gamma_2 &= 2.3; \\ V_{\max,2} &= V_2; & V_{\min,2} &= 0.1; & V_{0,2} &= 10. \end{aligned} \quad (45)$$

where  $T_a = 1\text{ms}$  was obtained from practical considerations in accordance with the response time allowed by the measurement and actuator subsystems.

The time evolution of the sliding variables  $\sigma_1$  and  $\sigma_2$  obtained using the fixed-gains and adaptive controllers are depicted in Fig. 5. The fixed-gains and the time-based adaptive controllers achieved the desired objectives, steering to and confining the sliding variables within a vicinity of zero in both cases. However, a significant chattering reduction can be appreciated when the adaptive controller is employed.

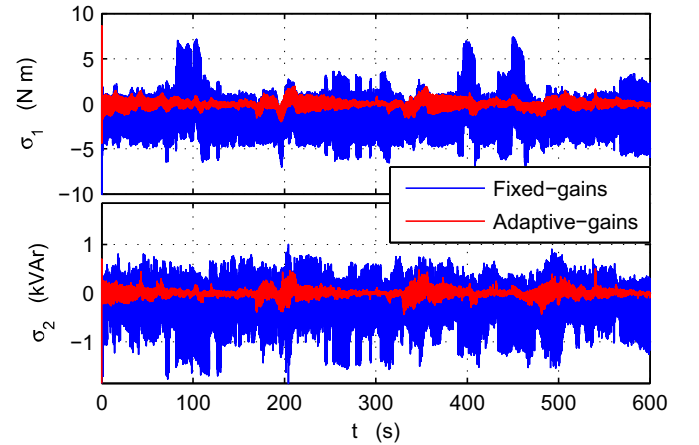


Figure 5. Sliding variables with the fixed-gains controller and the adaptive controller.

Note that tuning the gains large enough to deal with the uncertainties and disturbances in a wide operating range has another negative effect on the fixed-gains controller performance, besides of the aforementioned output chattering. This is the generation of severe mechanical efforts, that can be inferred from its broad torque variations in Fig. 6.

Counteracting the rate of variation of the generator torque is of paramount importance to increase the lifetime of the



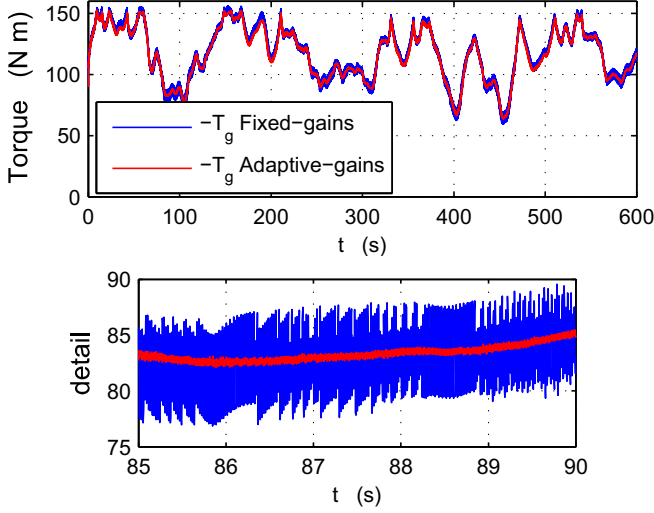


Figure 6. Torque with the fixed-gains controller and the adaptive controller (for whole time range on top and a detail in the lower plot).

WECSs. Evidently, this could be attained with the fixed-gains controller by reducing its gains, but at the expense of narrowing its robustness region and with the incorporation of an additional action into the control law, responsible to drive the system inside that region. On the other hand, without range reduction, it can be observed that the adaptive 2-SM controller provides in fact a remarkable attenuation of the generator torque vibrations (see detail in Fig. 6).

#### B. Noise and discretization effects

To validate the performance of the adaptive suboptimal controller in a more realistic scenario, measurement noise have been included in a further series of tests. Particularly, different simulation runs have been made by varying the noise level from 1% to 3% of the measurement range. Figure 7 depicts the obtained time evolutions of the sliding variables  $\sigma_1$  and  $\sigma_2$ , showing the corresponding progressive deterioration of the sliding accuracy when the measurement noise is considered. A continuous dependence of the sliding accuracy on the noise magnitude is observed.

Figure 8 depicts the actual and reference profiles of the generator torque (upper plot) and of the stator reactive power (lower plot), showing that very good tracking is attained by the proposed controller also in the presence of noise. It is worth to point out a slight deterioration of the generator torque tracking accuracy at  $t \geq 300$  (i.e., when the friction torque is added). The tracking precision, however, remains satisfactory. Short transient peaks can be seen in the  $Q_s$  profile at the transition times between operating zones.

Figure 9 displays the control voltage derivatives  $\dot{u}_1 = \frac{dv_{qr}}{dt}$  (upper plot) and  $\dot{u}_2 = \frac{dv_{dr}}{dt}$  (lower plot), showing the continuous adjustment of their magnitude provided by the adaptive 2-SMC scheme to face the variation of the uncertain drift and control gain terms. Figure 10 displays the corresponding applied control voltages  $u_1 = v_{qr}$  and  $u_2 = v_{dr}$ , which appear to be immune to chattering.

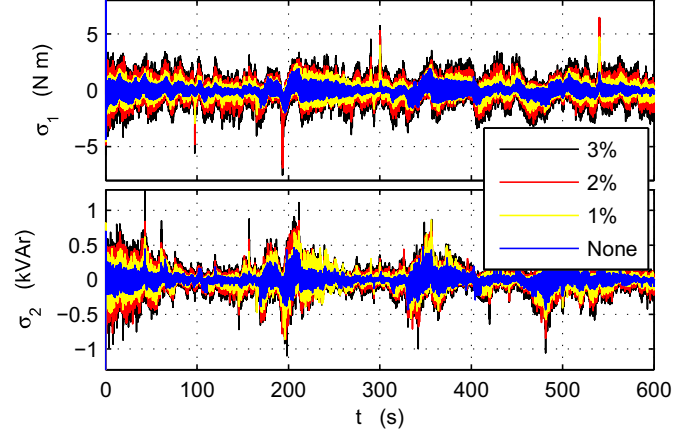


Figure 7. Sliding variables when different magnitudes of measurement noise is considered.

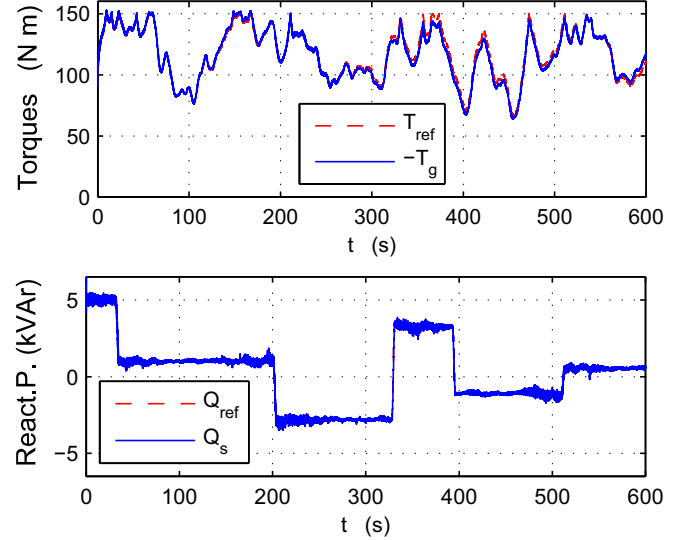


Figure 8. Upper plot: Actual and reference generator torque. Lower plot: Actual and reference stator reactive power. (Simulations considering measurement noise).

The sensitivity of the adaptive controller against the choice of the sampling period  $T_a$  is investigated next. Since the proposed adaptation mechanism counts the number of sign commutations of the sliding variable, it is expected that in the presence of noise selecting a too small value for  $T_a$  will yield the failure of the adaptation. Related analysis were made in [39], where the sensitivity of the TW algorithm to the presence of noise was under investigation and led to the important result that the sampling period should be selected proportional to the square root of the measurement noise magnitude since accuracy deterioration is observed using smaller values. The same result readily translates to the present scenario, since the suboptimal algorithm is homogeneous and the proposed adaptation is based on the sign of the sliding variable (in analogy with the TW controller). The proportionality constant is hard to compute and trial-and-error is needed in practice to properly tune the  $T_a$  parameter. Next simulations clearly show this fact. Figure 11 depicts the adaptive gains corresponding



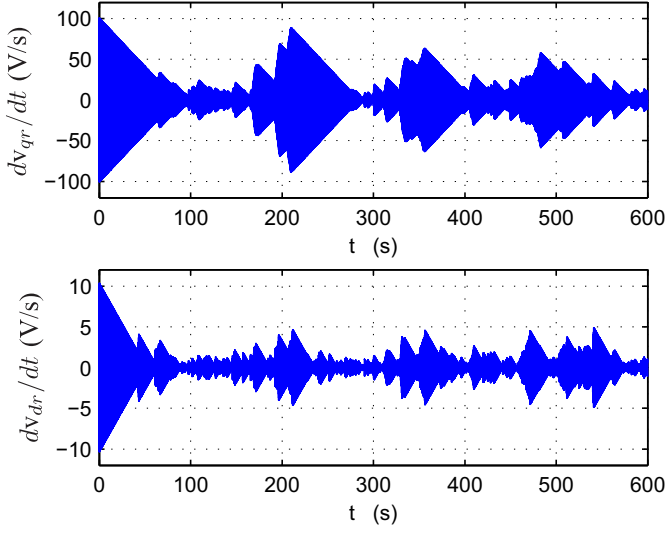


Figure 9. Control voltages derivatives:  $\dot{u}_1 = \frac{dv_{qr}}{dt}$  (upper plot) and  $\dot{u}_2 = \frac{dv_{dr}}{dt}$  (lower plot). (Simulations considering measurement noise).

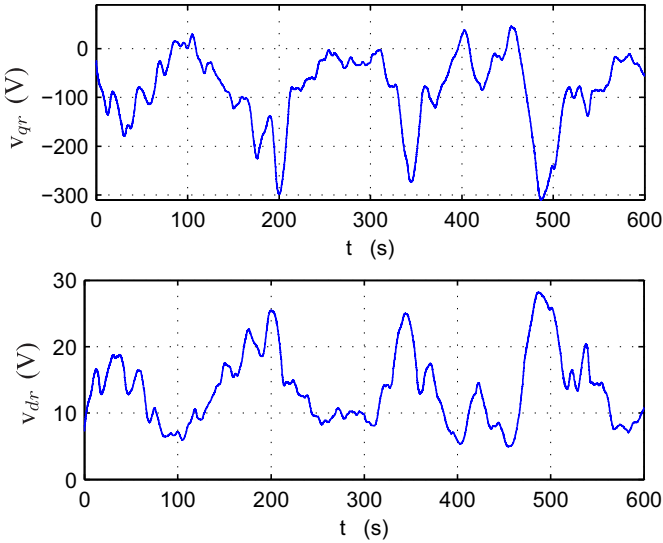


Figure 10. Control voltages:  $u_1 = v_{qr}$  (upper plot) and  $u_2 = v_{dr}$  (lower plot). (Simulations considering measurement noise).

to different tests where reduced values for  $T_a$  as compared to the value  $T_a = 1ms$  used in all the previous simulations were used. It can be seen that the smallest value  $T_a = 0.1ms$  leads to the failure of the gain adaptation in both the torque and reactive power control loops.

Overall, all presented tests have shown that the proposed adaptation mechanism is a practical solution, rather simple and easy to implement, to address the high performance control of a WECS under significant uncertainty effects and bringing considerable improvements as compared to the corresponding fixed-gains counterpart.

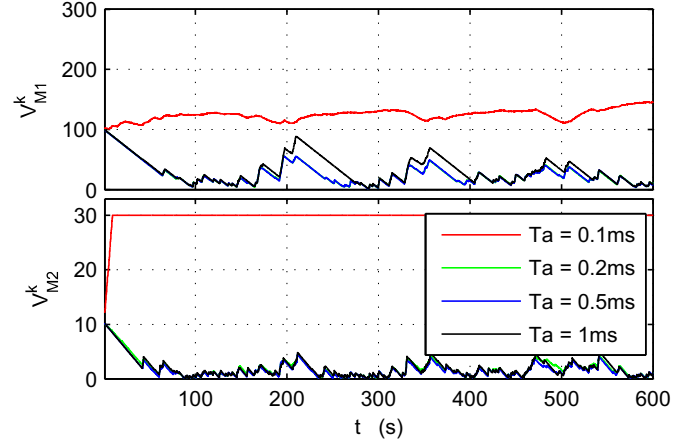


Figure 11. Adjustments of the amplitude parameter of the gains,  $V_{tb,1}(t) = V_{M1}^k$  and  $V_{tb,2}(t) = V_{M2}^k$ , for smaller adaptation periods of the gains,  $T_a$ , with measurement noise.

## VI. CONCLUSIONS

A robust controller setup for power conversion maximization and reactive power regulation of wind turbines was designed. To this end, an existing adaptive second-order sliding mode control scheme has been revisited in order to deal with quickly-varying disturbances (such as those present in WECSs), and its theoretical foundation was demonstrated. After thorough simulation tests, the novel time-based adaptive WECSs controller has shown satisfactory performance and robustness attesting not only the potential applicability of this combined control technique in the area of wind energy technology, but also its general applicability to non-linear systems subjected to fast varying uncertainty sources.

The critical issue of the selection of the  $T_a$  parameter should be kept in mind while tuning the control system, and particularly the variable measurement step strategy suggested in [39], suitably tailored to the present scenario, could be usefully implemented to further robustify the proposed controller. This issue will be investigated in our next research.

This research is the preliminary stage of a broader project aiming to implement and compare several adaptive 2-SM controllers in a real small-scale wind turbine (10-60kW), to optimise energy capture and extend its service life.

## APPENDIX A PROOF OF THEOREM 1

Unlike the initial conditions already belong to a close vicinity of the origin of the  $z_1Oz_2$  plane, during the initial transient there are no frequent sign commutations of  $\omega(t)$  and, hence, the time-based magnitude  $V_{tb}(t)$  will start increasing from its initial value  $V_0$  and two possible scenarios can arise.

In one of them,  $V_{tb}(t)$  will reach the maximum value  $V_{max}$ , and then keep constant. Then, according to the convergence properties of the fixed-gains version of the Suboptimal algorithm, the resulting trajectories will start to converge towards the origin.

While approaching the origin, the contraction condition  $|z_{1M,h+1}| \leq \gamma |z_{1M,h}|$  ( $\gamma < 1$ ) is enforced by the Suboptimal

algorithm, and the frequency of the sign commutations of  $\omega(t)$  will progressively increase. Theoretically, the frequency of sign commutations of  $\omega(t)$  tends to infinity while approaching the origin. Hence, the real-sliding criterion (37) is fulfilled at some  $k = M_1$ , and the stepwise reduction of  $V_M^k$  will be then activated starting from the end of the time interval  $\mathcal{T}_{M_1}$ .

In the other possible, and more favorable, scenario,  $V_{tb}(t)$  will be growing during the initial transient but the real-sliding criterion (37) will be already achieved before that  $V_{tb}(t)$  reaches the maximum value  $V_{\max}$ . Also in this case, the stepwise reduction of  $V_M^k$  will be activated starting from the end of some time interval  $\mathcal{T}_{M_1}$ .

The gain dominance condition (31) can be specialized to a restricted time interval  $\mathcal{T}_k$  as follows

$$V_{\max} > \Phi N_k, \quad N_k = \sup_{t \geq \mathcal{T}_k} |\eta(t)| \leq F/G_m. \quad (46)$$

By relying on the fact that  $N_{sw}^{M_1}(\omega) \geq N^*$ , there is  $\tau_1 \in \mathcal{T}_{M_1}$  such that the time-based adaptive control gain  $V_{tb}(M_1 T_a) = V_M^{M_1}$  will be dominating the actual upper bound of  $|\eta(\tau)|$ , in accordance with (46), as

$$V_M^{M_1} \geq \Phi |\eta(\tau_1)|, \quad \tau_1 \in \mathcal{T}_{M_1}. \quad (47)$$

Starting from the end of the time interval  $\mathcal{T}_{M_1}$ , the process of reducing the control gain is activated, i.e.,  $V_M^{M_1+\ell} = V_M^{M_1+\ell-1} - \Lambda T_a$ ,  $\ell = 1, 2, \dots$ . Thus, the dominance over the uncertainties (formalized by condition (47)) will be lost after a finite number of intervals, and there is  $M_2 > M_1$  such that at  $k = M_2$  the real-sliding criterion (37) will be violated. It implies that along the preceding time interval  $\mathcal{T}_{M_2-1}$  a dominance inequality analogous to (47) holds:

$$V_M^{M_1} \geq \Phi |\eta(\tau_2)|, \quad \tau_2 \in \mathcal{T}_{M_2-1}. \quad (48)$$

By Lemma 1, along the time interval  $\mathcal{T}_{M_2-1}$  the variables  $z_1$  and  $z_2$  are bounded as in (38) with

$$\rho_1 = \sup_{t \in \mathcal{T}_{M_2-1}} |\dot{z}_2(t)| = G_M [N_{M_2-1} + V_M^{M_2-1}]. \quad (49)$$

Along the interval  $\mathcal{T}_{M_2+1}$ , i.e. one interval after the violation of the 2-sliding criterion (37), the magnitude of the uncertainty  $\eta(t)$  will be such that

$$|\eta(\tau_3)| \leq |\eta(\tau_2)| + 3PT, \quad \forall \tau_3 \in \mathcal{T}_{M_2+1}, \quad (50)$$

which is derived by taking into account (40). On the other hand, the adaptive magnitude will be increased at the end of the interval  $\mathcal{T}_{M_2-1}$ , and decreased at the end of the successive interval  $\mathcal{T}_{M_2+1}$ , which means that

$$V_M^{M_2+1} > V_M^{M_2-1} + T(\Gamma - \Lambda). \quad (51)$$

Therefore, considering (48) and (50)-(51), if the  $\Gamma$  parameter is such that

$$\Gamma > \Lambda + 3P, \quad (52)$$

it follows that the dominance condition (46) will be already restored along the interval  $\mathcal{T}_{M_2+1}$ , i.e. one interval after the violation of the sliding mode existence criterion (37). While  $V_M^k$  continues to grow, which will happen for a finite number of adaptation intervals until the SM existence criterion (37)

will be restored, contractive rotations of the system trajectories in the  $z_1 - z_2$  plane will take place, which can be evaluated by studying the piecewise-parabolic limit trajectories of the Suboptimal algorithm (see [38]) starting from the initial condition (38). Lengthy, but straightforward computations show that the transient deviations of  $z_1$  and  $z_2$  fulfil inequalities analogous to (42), with the constants  $b_1$  and  $b_2$  independent of  $T$ . The process of loosing, and successively restoring, the dominance over the uncertainties will iteratively continue, thereby preserving inequalities (42). Theorem 1 is proved.  $\triangle$

## APPENDIX B

### INDUCTION GENERATOR FULL ORDER DYNAMICAL MODEL

The four nonlinear differential equations that together with (2), describe an induction generator in a synchronously rotating direct quadrature (d-q) frame are

$$\mathbf{v} = \mathbf{Z} \mathbf{i}, \quad (53)$$

$$\mathbf{Z} =$$

$$\begin{bmatrix} R_s + L_s \frac{d}{dt} & -\omega_s L_s & L_m \frac{d}{dt} & -\omega_s L_m \\ \omega_s & R_s + L_s \frac{d}{dt} & \omega_s L_m & L_m \frac{d}{dt} \\ L_m \frac{d}{dt} & -s\omega_s L_m & R_r + L_r \frac{d}{dt} & -s\omega_s L_r \\ s\omega_s L_m & L_m \frac{d}{dt} & s\omega_s L_r & R_r + L_r \frac{d}{dt} \end{bmatrix}$$

where  $\mathbf{v} = [v_{ds}; v_{qs}; v_{dr}; v_{qr}]^T$ ,  $\mathbf{i} = [i_{sd}; i_{sq}; i_{rd}; i_{rq}]^T$ ,  $\frac{d}{dt}$  is the time derivative operator, and  $L_m$  is the magnetizing inductance. All the rotor variables have been referred to the stator side by  $n_1$ . The equation for the generator torque, which replaces (5), is

$$T_g = p_p L_m (i_{sq} i_{rd} - i_{sd} i_{rq}). \quad (54)$$

Variables are referred to the fast shaft side by

$$T_t = \frac{T_{tlow}}{k_{gb}}; \quad \Omega_g = \Omega_{low} k_{gb}; \quad J = \frac{J_t}{k_{gb}^2} + J_g, \quad (55)$$

where  $J_t$  and  $J_g$  are the inertia of the turbine rotor and of the generator rotating parts respectively.

## APPENDIX C

### PARAMETERS OF THE DFIG BIDIRECTIONAL TOPOLOGY

Table II  
NOMINAL PARAMETERS OF THE DFIG BIDIRECTIONAL TOPOLOGY.

$P_r=37$ kW;	$R=7.3$ m;	$c_0=-0.1380$ ;
$\omega_s=2\pi 60$ $\frac{\text{rad}}{\text{s}}$ ;	$J=3.662$ kgm <sup>2</sup> ;	$c_1=0.0692$ ;
$V_s=375.6$ V;	$k_{gb}=25$ ;	$c_2=-0.0074$ ;
$p_p=2$ ;	$L_s=35.5$ mH;	$c_3=2.113 \cdot 10^{-4}$ ;
$R_s=82$ m $\Omega$ ;	$L_r=35.5$ mH;	$\lambda_{opt}=7.63$ ;
$R_r=228$ m $\Omega$ ;	$L_m=35.7$ mH;	$C_{p \max}=0.4018$ ;

## REFERENCES

- [1] "Small wind world report 2012," World Wind Energy Association, Tech. Rep., Mar 2012. [Online]. Available: <http://www.wwindea.org/>
- [2] I. Munteanu, A. Bratcu, N. Cutululis, and E. Ceanga, *Optimal Control of Wind Energy Systems*. Springer-Verlag London, 2007.
- [3] M. Garcia-Sanz and C. Houpis, *Wind Energy Systems: Control Engineering Design*. CRC Press, Taylor & Francis Group, 2012.
- [4] S. Emelyanov, *Variable Structure Control Systems*, Moscow, Nauka, 1967.

- [5] V. Utkin, "Variable structure systems with sliding modes," *IEEE Trans. Automat. Contr.*, vol. 22, no. 2, pp. 121–122, Apr. 1977.
- [6] A. Sabanovic, L. Fridman, and S. Spurgeon, Eds., *Variable Structure Systems: From Principles to Implementation*. IET, UK, 2004.
- [7] C. Edwards, E. Fossas Colet, and L. Fridman, Eds., *Advances in Variable Structure and Sliding Mode Control*. Berlin: Springer, 2006.
- [8] G. Bartolini, L. Fridman, A. Pisano, and E. Usai, Eds., *Modern Sliding Mode Control Theory: New Perspectives and Applications*. Springer, 2008, vol. 375.
- [9] Y. Shtessel, C. Edwards, L. Fridman, and A. Levant, Eds., *Sliding Mode Control and Observation*. New York: Springer, 2013.
- [10] A. Levant, "Sliding order and sliding accuracy in sliding mode control," *International Journal of Control*, vol. 58, no. 6, pp. 1247–1263, 1993.
- [11] L. Fridman and A. Levant, *Robust Control Variable Structure and Lyapunov Techniques*. London: Springer Verlag, 1996, no. 217, ch. 1 Higher order sliding modes as the natural phenomena of control theory, pp. 107–133.
- [12] G. Bartolini, A. Ferrara, A. Levant, and E. Usai, *Variable Structure Systems, Sliding Mode and Nonlinear Control*. Springer, 1999, ch. 17 "On Second-Order Sliding-Mode Controllers", pp. 329–350.
- [13] A. Pisano and E. Usai, "Sliding mode control: A survey with applications in math," *Mathematics and Computers in Simulation*, vol. 81, no. 5, pp. 954 – 979, 2011.
- [14] H. Lee and V. Utkin, "Chattering suppression methods in sliding mode control systems," *Annual Reviews in Control*, vol. 31, pp. 179–188, 2007.
- [15] F. Plestan, Y. Shtessel, V. Bregeault, and A. Poznyak, "New methodologies for adaptive sliding mode control," *International J. of Control*, vol. 83, pp. 1907–1919, 2010.
- [16] Y. Shtessel, J. Moreno, F. Plestan, L. Fridman, and A. Poznyak, "Super-twisting adaptive sliding mode control: A Lyapunov design," in *Decision and Control (CDC), 2010 49th IEEE Conference on*, Dec. 2010, pp. 5109–5113.
- [17] T. Gonzalez, J. Moreno, and L. Fridman, "Variable gain super-twisting sliding mode control," *IEEE Trans. Automat. Contr.*, vol. 57, no. 8, pp. 2100–2105, 2012.
- [18] C. Evangelista, P. Puleston, F. Valenciaga, and L. Fridman, "Lyapunov designed super-twisting sliding mode control for wind energy conversion optimization," *IEEE Transactions on Industrial Electronics*, vol. 60, pp. 538–545, 2013.
- [19] C. Evangelista, F. Valenciaga, and P. Puleston, "Active and reactive power control for wind turbine based on a mimo 2-sliding mode algorithm with variable gains," *IEEE Transactions on Energy Conversion*, vol. 28, pp. 682–689, 2013.
- [20] V. Utkin and A. Poznyak, "Adaptive sliding mode control with application to super-twisting algorithm: Equivalent control method," *Automatica*, vol. 49, pp. 39–47, 2013.
- [21] C. Edwards and Y. Shtessel, "Dual-layer adaptive sliding mode control," in *American Control Conference (ACC), 2014*, 2014, pp. 4524–4529.
- [22] —, "Adaptive dual layer second-order sliding mode control and observation," in *American Control Conference (ACC), 2015*, 2015, pp. 5853–5858.
- [23] Y. Shtessel, M. Taleb, and F. Plestan, "Lyapunov design of adaptive super-twisting controller applied to a pneumatic actuator," in *IFAC World Congress, 2011*, 2011, pp. 3051–3056.
- [24] Y. Shtessel, M. Taleb, and Plestan, "A novel adaptive-gain super-twisting sliding mode controller: methodology and application," *Automatica*, vol. 48, pp. 759–769, 2012.
- [25] Y. Shtessel, J. Kochalummootti, C. Edwards, and S. Spurgeon, "Continuous adaptive finite reaching time control and second order sliding modes," *IMA J. of Mathematical Control and Information*, vol. 30, pp. 97–113, 2013.
- [26] A. Levant, M. Taleb, and Plestan, "Twisting-controller gain adaptation," in *Conference on Decision and Control (CDC), 2011*, 2011, pp. 7015–7020.
- [27] F. Plestan, Y. Shtessel, V. Bregeault, and A. Poznyak, "Sliding mode control with gain adaptation -application to an electropneumatic actuator," *Control Engineering Practice*, vol. 21, pp. 679–688, 2013.
- [28] G. Liu, A. Zinober, Y. Shtessel, and Q. Niu, "Adaptive twisting sliding mode control for the output tracking in time delay systems," *Australian J. of Electrical and Electronics Engineering*, vol. 9, pp. 217–224, 2012.
- [29] J. Kochalummoottil, Y. Shtessel, J. Moreno, and L. Fridman, "Adaptive twist sliding mode control: a lyapunov design," in *Conference on Decision and Control (CDC), 2011*, 2011, pp. 7623–7628.
- [30] —, "Output feedback adaptive twisting control: A Lyapunov design," in *American Control Conference (ACC), 2012*, June 2012, pp. 6172–6177.
- [31] G. Bartolini, A. Levant, A. Pisano, and E. Usai, "2-sliding mode with adaptation," in *Procs. 7th IEEE Mediterranean Conference on Control and Systems*, Haifa, Israel, 1999.
- [32] L. Capisani, A. Ferrara, and A. Pisano, "Second-order sliding mode control with adaptive control authority for the tracking control of robotic manipulators," in *18th IFAC World Congress*, Italy, 2011.
- [33] A. Pisano, M. Tanelli, and A. Ferrara, "Time-based switched sliding mode control for yaw rate regulation in two-wheeled vehicles," in *Decision and Control (CDC), 2012 IEEE 51st Annual Conference on*, Dec. 2012, pp. 0743–1546.
- [34] —, "Combined switched/time-based adaptation in second order sliding mode control," in *Decision and Control (CDC), 2013 IEEE 52nd Annual Conference on*, 2013, pp. 4272–4277.
- [35] C. Evangelista, A. Pisano, P. Puleston, and E. Usai, "Time-based adaptive second order sliding mode controller for wind energy conversion optimization," in *53rd IEEE Conference on Decision and Control - CDC 2014*, Los Angeles, US, Dec. 2014.
- [36] T. Burton, D. Sharpe, N. Jenkins, and E. Bossanyi, *Wind Energy handbook*. England: John Wiley and Sons, 2001.
- [37] I. Erlich and F. Shewarega, "Modeling of wind turbines equipped with doubly-fed induction machines for power system stability studies," in *Power Systems Conference and Exposition, 2006 IEEE PES*, 2006, pp. 978–985.
- [38] G. Bartolini, A. Ferrara, A. Pisano, and Usai, "On the convergence properties of a 2-sliding control algorithm for non-linear systems," *International Journal of Control*, vol. 74, no. 7, pp. 718–731, 2001.
- [39] A. Levant, "Variable measurement step in 2-sliding control," *Kybernetika*, vol. 36, pp. 77–93, 2000.



**Carolina A. Evangelista** received the Engineers degree in electronics and the Ph.D. degree from the Universidad Nacional de La Plata (UNLP), La Plata, Argentina, in 2006 and 2012, respectively.

She is a Researcher since 2013 with CONICET and UNLP, at the LEICI Institute, Argentina. She is currently a Professor teaching Control Theory at the Information Systems Engineering Department, UTN, and a Teaching Assistant in Control and Automation at the Department of Electrical Engineering, UNLP. Her research interests are in high order sliding mode

control, with applications in renewable energy systems (mainly wind, fuel cells and marine waves based) and, lately, in mechanical lung ventilation.



**Alessandro Pisano** was born in 1972. He graduated in Electronic Engineering in 1997 at the Department of Electrical and Electronic Engineering (DIEE) of the Cagliari University (Italy), where he received the Ph.D. degree in Electronics and Computer Science in 2000.

He currently holds a permanent position as Assistant Professor at DIEE. His current research interests include nonlinear control theory and its application to control, observation and fault detection of nonlinear, uncertain and/or distributed parameter systems.

He has authored/co-authored one book, 62 journal publications, 10 book chapters, and in excess of 100 papers in peer-reviewed international conference proceedings, and he is the holder of 4 patents. He has spent long-term visiting periods at Universities and Research Centers in Belgium, France, Serbia and Mexico.

He is a member of IEEE and a Professional Engineer registered in Cagliari, Italy. He is Associate Editor of the Asian Journal of Control and of the IEEE Control Systems Society Conference Editorial Board.



**Paul Puleston** received his Electronic Engineering degree (with first class Hons.) and his Ph.D. degree from the Universidad Nacional de La Plata (UNLP), Argentina, in 1988 and 1997, respectively.

He is currently Full Professor at the Department of Electrical Engineering, FI-UNLP, Vice Director of the LEICI and Researcher of CONICET, Argentina. His main research field is automatic control systems, theory and applications, including alternative energy systems.



**Elio Usai** (M96) received the M.Sc. Degree in electrical engineering from the University of Cagliari, Cagliari, Italy, in 1985.

He was a Process Engineer and then a Production Manager for international companies. In September 1994, he joined the Department of Electrical and Electronic Engineering (DIEE), University of Cagliari, where he is currently Professor. He has been the leader of research projects on the control of uncertain systems and on model-based fault detection. He has coauthored over 150 articles published in international journals and conference proceedings. His current interests are in output-feedback control, state estimation, and FDI via higher order sliding modes in linear, nonlinear, and infinite dimensional systems.

Elio Usai was the General Chairperson of the 2006 International Workshop on Variable Structure Systems. He is currently an Associate Editor of the Asian Journal of Control, the IEEE Transactions on Control Systems Technology and the Journal of the Franklin Institute.